

Electrostatic forces and micromanipulator design: on the importance of surface topography parameters

Marion Sausse Lhernould, Alain Delchambre, Stéphane Régnier and Pierre Lambert

Abstract—Micro manipulations of objects between 10 μm and 1 mm by contact are often disturbed by the surface forces appearing between the handled object and the gripper. They may overcome gravity and prevent the release of the object. Capillary, electrostatic and van der Waals forces are the main surface forces responsible for this adhesive phenomenon. Several factors may influence these forces such as the materials in contact, the fabrication process, the surface treatments or the surface contaminations. All of these contribute to shape the topography of the surface. In this paper is investigated in which way surface roughness could be used to overcome the problem of adhesive electrostatic forces. Simulations are performed for smooth surfaces and for rough surfaces in order to study the influence of surface topography. The simulation tool is validated using analytical models for the smooth case and shows a good correlation. Roughness is modeled using a fractal representation (Weierstrass-Mandelbrot function). The simulations using fractal representation show a significant influence of the surface topography at small separation distances and correlate experimental benchmarks from literature. Topography of the surface should not be neglected in micromanipulator design.

Index Terms—adhesion, electrostatic forces, roughness, fractals.

I. INTRODUCTION

Micro manipulations of object between 10 μm and 1 mm by contact are often disturbed by the sticking of the handled object on the manipulator. Capillary, electrostatic and van der Waals forces are the main surface forces responsible for this adhesive phenomenon. They have already been studied in previous works [1], [2], [3], [4]. It has been observed that they may be influenced by several factors such as the materials in contact, the fabrication process, the surface treatments and the surface contaminations. These factors shape the topography of the contacting surface. No matter how carefully or expensively the surface is manufactured it can never be perfectly smooth. This roughness may decrease the adhesion forces due to the reduction of the surface of contact [5].

Due to capillary condensation, a liquid film can form between two objects in contact (e.g. the gripper and the handled object in micromanipulation experiments). From the formation of this meniscus results a capillary force that can make a large contribution to the total adhesion

Manuscript received January 12, 2007.

This work has been supported by a grant from the Communauté Française de Belgique (ARC 04/09-310).

M. Sausse Lhernould, A. Delchambre and P. Lambert are with the Bio Electro And Mechanical Systems Department, Université Libre de Bruxelles (ULB), Bruxelles, Belgium (corresponding author phone: +32 2 650 29 31; fax: +32 2 650 47 24; e-mail: msausse@ulb.ac.be).

S. Régnier is with Laboratoire de Robotique de Paris, Université Pierre et Marie Curie (UPMC), Fontenay aux Roses, France.

force [6]. With hydrophilic surfaces the meniscus force increases for smoother surfaces so that the adhesion of ultra-flat surfaces can be extremely strong [7]. A significant decrease in the magnitude of the adhesion force with an increase in roughness in the low relative humidity regime has been observed [8] demonstrating that capillary adhesion is substantially lowered in the presence of nanoscale roughness. The Van der Waals forces are due to the instantaneous polarization of the atoms and molecules due to quantum mechanical effects. In the case of two rough surfaces the average inter-planar distance would be large and the van der Waals forces would be small [7]. These forces depend greatly on the roughness of the surface.

The focus is here on the electrostatic forces because they are the most significant force for grasping and manipulating parts between 10 μm and 1 mm [5]. They can be active over ranges of the order of the object radius. Electrostatic forces alone can already be significant enough to perturb the manipulation of micro-objects. A perspective of this work is to include other surface effects. Simulations are performed using the finite element software Comsol in order to determine the importance of roughness in the adhesive phenomenon. The interest of developing such a simulation tool is for applications to micromanipulator design. The idea is to answer two questions. Could adhesive electrostatic forces be significantly decreased with a specific fabrication process or treatment? How to choose the best fabrication solution for microgrippers?

The paper is divided into five main sections. The next one deals with roughness representation, the available models and a discussion about the fractal representation (which is the one chosen in this work). The third section deals with the electrostatic forces and the simulations showing their correlation with analytical models and literature benchmark. Section four shows how surface topography may be included in micromanipulator design before concluding.

II. ROUGHNESS REPRESENTATION

A. Roughness models

Many authors agree that even a nanoscale roughness should be taken into consideration when performing simulations of adhesion [9]. Finding accurate models for surface topography representation is of crucial importance. The most often encountered models in the literature are presented in the following.

The simplest case [10] only considers the roughness peaks. The roughness profile is assumed to be equivalent to a smooth profile located at a separation distance $d+R/2$, where

R is the height of the highest peak and d is the distance between the plane and the highest peak (Figure 1). This model is however not accurate since it does not take into account the density of protrusions.

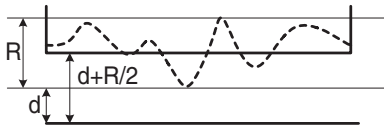


Fig. 1. Planar model [10]

Elementary protuberances such as hemispheres and cones (Figure 2) may also be used to model the asperities. Usually the roughness is modeled as hemispherical asperities characterized by the average asperity height and the density of asperities on the surface. This type of representation is found in [11], [12], [13].



Fig. 2. Hemispherical asperities [11]

A third technique uses sinusoidal functions. A cosine function is used in [14] which is an idealized periodic surface characterized by shape, height and wavelength to calculate the electrostatic repulsive energy between two rough colloidal particles.

Finally a last technique involves the use of fractals. The reader is referred to the next section for details. This model is used for our own simulations. Indeed the topography of many engineered surfaces may be represented as fractals [15] because similar features can be observed at different magnification of the same surface. It is necessary to characterize rough surfaces by intrinsic parameters which are independent of all scales of roughness such as the fractal parameters [16].

B. The fractal representation

Fractals are irregular objects possessing similar geometrical characteristics at all scales, i.e. self-similarity characteristics. The geometries of fractal surfaces are also continuous and non differentiable. Since the profile of rough surfaces $z(x)$ (typically obtained from stylus measurements) is assumed to be continuous even at the smallest scales and ever-finer levels of detail appear under repeated magnification, the tangent at any point cannot be defined. The profile has thus the mathematical property of being continuous everywhere but non-differentiable at all points. The Weierstrass-Mandelbrot function satisfies the properties of continuity, non-differentiability and self-similarity [17] and is therefore used to simulate two-dimensional profiles.

$$z(x) = L \left(\frac{G}{L} \right)^{D-1} \sum_{n=0}^{\infty} \frac{\cos(2\pi\gamma^n \frac{x}{L})}{\gamma^{(2-D)n}} \quad (1)$$

where L is the fractal sample length, D is the fractal dimension ($1 < D < 2$), G is the fractal roughness parameter and γ is a scaling parameter ($\gamma > 1$). Equation 1 models the surface profile by a sum of cosine functions with geometrically increasing frequencies. In order for the phases of the different modes not to coincide at any given x position, the value of γ must be chosen to be a non integer (it is good to assume $\gamma=1.5$ [18]). As D becomes larger, the number of asperities increases (density increases) and their height decreases. As G increases, the peaks and the valleys are amplified. As the magnitudes of D and G increase, a rougher and more disordered surface topography can be generated. Figure 3 illustrates the influence of the fractal parameters D and G on the generated profile.

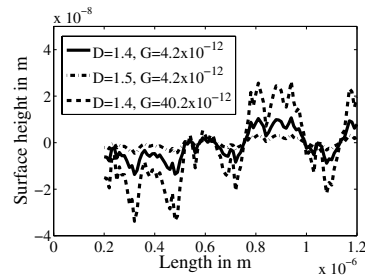


Fig. 3. Influence of the fractal parameters on the generated profile.

Fractal representation of surface roughness has however often been debated and authors do not all agree about its relevance. The main problem that has been suggested with using fractal representation for the topography of engineered surfaces is that not all of these surfaces are fractal. The fractal character of artificial surfaces depends on the processing method ([19], [20]). For [21], fractals may not be applicable to very smooth surfaces. The scale independence of the fractal parameters has been questioned in [19], [21], [22]. On the other hand, [15] many engineered surfaces can be represented by fractals. It has been shown that surfaces of processed steel, textured magnetic thin film [23], and metallic surfaces produced by EDM, by cutting or grinding techniques, and even worn surfaces [24] are fractal. Arguments in favor of the fractal characterization can be summarized by the necessity to characterize rough surfaces using intrinsic parameters independent of all scales.

III. SIMULATIONS

A. Description

During micromanipulations the contact potential difference (CPD) between the gripper and the manipulated object depends on the intrinsic properties of the materials in the case of conducting materials. Electrons in a metal have a certain energy level and stay in the metal at rest. There is a minimum energy level defined for each metal that its electrons have to acquire in order to be able to leave it. This energy is defined as the work function. Two pieces of different metals placed sufficiently close to exchange electrons will reach thermodynamic equilibrium by equalizing the height of their

Fermi levels. Equilibrium is reached by the establishment of the contact potential. The result is an attractive electrostatic force between the objects in proximity. The electric potential U in the surrounding environment obeys Laplace's equation:

$$\Delta U = 0, \quad (2)$$

The electric field is obtained from the gradient of U .

$$\vec{E} = -\nabla U \quad (3)$$

Simulations are done for the configuration of a contact between an object and a flat surface representing the gripper end-effector. The two-dimensional axisymmetric simulation is performed using the commercial simulation tool Comsol to model the geometry and to solve the partial differential equation (Equation 2) using the finite element method. The outer boundary conditions modeling the surrounding environment are placed sufficiently away to consider that no charges are present on them. The potential U is applied on the boundary delimiting the contacting object while the contacting flat surface (corresponding to the gripper) is grounded. The electrostatic forces are calculated using Equation 4.

$$F_{elec} = \frac{\epsilon_0 \epsilon_R E^2}{2} \quad (4)$$

where ϵ_R is the relative permittivity of the medium ($\epsilon_R = 1.00054$ in air) and ϵ_0 is the permittivity of free space ($\epsilon_0 = 8.85 \times 10^{-12}$ F/m). Integrating the force for all of the elements in the model, we are able to calculate the total force acting on the two geometries.

B. Comparison with analytical results

The simulations have been validated using analytical models from the literature. In these models the main assumption is that the surfaces are completely smooth. The second assumption is that the materials are conductive which involves that the potential is uniformly distributed along the surface, the electric field is normal to the surfaces and the charges only carried by the surfaces of the materials (no volume charges). No charge is present between the contacting objects meaning that the charges are only present at the surfaces of the materials. Two types of contacts have been used: sphere-plane and cone-plane because they are the most used in literature particularly in predicting electrostatic forces in atomic force microscopy. For the sphere-plane contact the expressions developed by [25], [26], [27] were used. Results are presented in Figure 4. For the cone-plane contact works from [28], [29] were used. Results are presented in Figure 5.

C. Comparison with experimental results

Available experimental measures of the electrostatic forces have all been realized at the nanoscale in the framework of scanning probe microscopy. Sacha et al.'s work [30] is used to compare results of our simulations with their experimental results. They measured electrostatic forces for a sphere-ended conical tip of radius 40 nm and half aperture angle 20° for

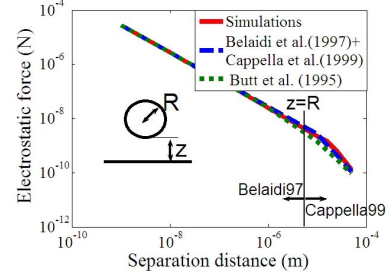


Fig. 4. Validation of simulations with the sphere models (Belaidi et al. [25] and Cappella et al. [26] distinguish $z < R$ and $z > R$ while model from Butt et al. [27] is given for all distances), for a sphere of radius $10\mu\text{m}$ and a potential difference $U=10\text{V}$.

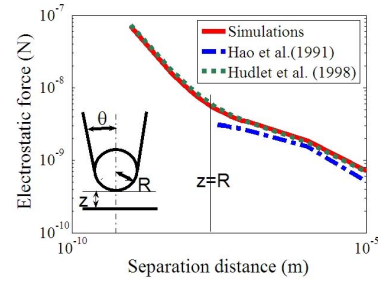


Fig. 5. Validation of simulations with the models using conical geometries for dimensions of the tip $L=125\mu\text{m}$, $R=25\text{nm}$, $\theta=9.46^\circ$ (half aperture angle) and a potential difference $U=10\text{V}$ with the asymptotic model from Hudlet et al. [28] and the uniformly charged line model from Hao et al. [29].

different voltages (6, 8 and 10V). The characteristics of the tip were found using SEM images. The sample was a gold-coated glass slide. Their results were compared with the simulations, first without and then with roughness included (fractal representation). Figure 6 gives a representation of the contact between the conical tip and the rough surface generated using a Weierstrass Mandelbrot function during simulations (axisymmetric problem).

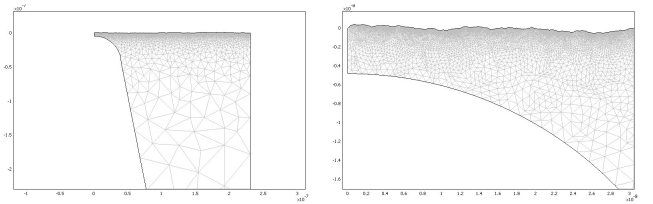


Fig. 6. Visualization of the mesh for a simulation of the contact between a conical sphere ended tip and a rough surface.

First observations were that even though the results are in good correlation for smooth simulations, simulated forces are stronger than what was obtained experimentally. The difference between experimental results and simulations increases when the separation distance decreases. We attributed this observation to the fact that even though the spot of contact has been chosen to be smooth (atomic steps), it can never

be perfectly smooth. A very small roughness may influence the results at such small separation distances. Results are presented in Figure 7. We introduced roughness with the

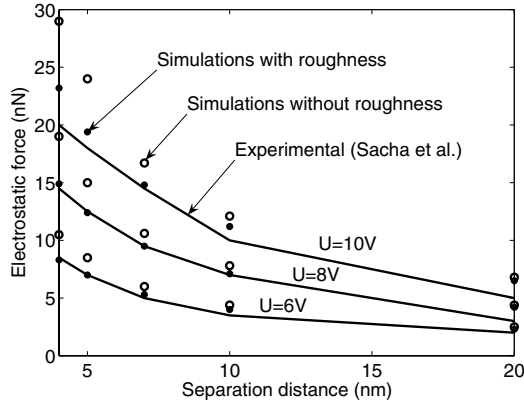


Fig. 7. Electrostatic normal force (nN) versus separation distance(nm) for different applied voltages for a sphere-ended conical tip of radius 40nm and half aperture angle $\theta=20^\circ$. Plot shows experimental results obtained by Sacha et al. [30], simulations results without roughness parameters and simulation results including roughness parameters $G = 5 \times 10^{-11}$ and $D = 1.8$ chosen in order to get an arithmetic average roughness of the order of 0.4nm

generation of a fractal surface using fractal parameters $D=1.8$ and $G = 5 \times 10^{-11}$ for the planar contacting surface in order to have an arithmetic average roughness of 0.4nm (which is often assumed to be negligible).

Even a roughness as small as the one simulated is influencing the results from simulations by reducing the electrostatic forces. This is specially true when the tip gets closer to the surface. The influence of surface roughness is also more important at higher applied voltages. The results from our simulations including roughness are closer to the experimental measures. From these observation it is believed that surface topography is an important parameter in predicting electrostatic forces. It reflects the materials, the fabrication process and surface treatment and should not be neglected. Roughness decreases the electrostatic forces. In application to micromanipulator design roughening may thus be a solution to avoid adhesive effect of electrostatic forces. This is investigated in the next section

IV. SURFACE TOPOGRAPHY IN DEVELOPING DESIGN SOLUTIONS FOR CONTACT MICROMANIPULATORS

In this part the simulation tool is used for simulations of a contact between a spherical object with an infinite plane. The arithmetic average roughness R_a was chosen as reference parameter even if the representation is fractal and the roughness parameters are thus D and G (Equation 1). Speaking in terms of fractal parameters would however not have been very representative to the reader. Using the arithmetic average roughness gives a better qualitative view on the effect of surface roughness.

Figure 8 shows the influence of the object radius on the electrostatic force for different average arithmetic rough-

nesses of the contacting plane. As expected higher roughness leads to smaller electrostatic forces. Even though the influence of roughness seems to remain similar for all radius values (curves are almost parallel), the effect of roughness is more noticeable on higher object radius. The ratio between forces in the smooth configuration and forces in the rough configuration is increased when the object radius increases. Figure 9 shows that roughness is an important parameter that influences the electrostatic forces not only at contact. Even an average arithmetic roughness as small as 4 nm decreases the electrostatic forces at separation distance up to 50 nm.

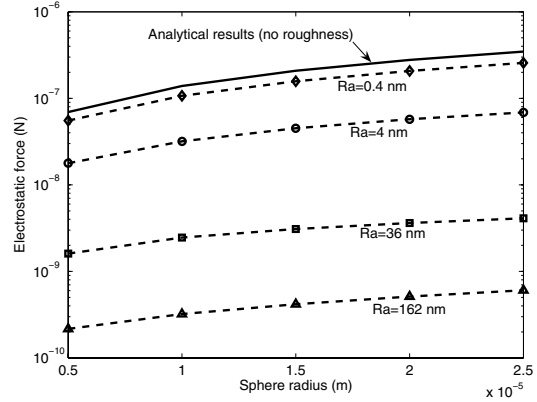


Fig. 8. Electrostatic normal force (N) versus object radius (m) for different roughnesses R_a for a spherical object in contact with an infinite plane. Potential U is 0.5 V and separation distance z is 0.5 nm.

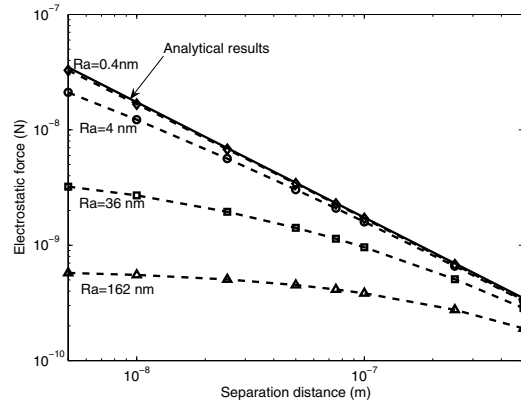


Fig. 9. Electrostatic normal force (N) versus separation distance (m) for different roughnesses R_a for a spherical object in contact with an infinite plane. Potential U is 0.5 V and radius R is 25 μm .

Simulations of a contact between a spherical object of radius $R=25\mu\text{m}$ and an infinite plane are also performed in order to evaluate the feasibility of the release. Contact occurs at the inter-atomic separation distance between surfaces which is 0.5 nm [31]. The material considered for the spherical object is steel ($\rho = 7800\text{kg}/\text{m}^3$). The electrostatic forces are simulated at contact for different arithmetic average roughnesses of the plane (R_a between 1

nm and 31 nm). Results are presented in Figure 10. From these we observe that for a contact potential difference (CPD) of 0.1 V, there will be no problem in releasing the object if the arithmetic average roughness is a least 2 nm because gravity will overcome the electrostatic forces. For a CPD of 0.3 V there may be a problem of adhesion due to electrostatic forces except if the plane has an arithmetic average roughness of at least 13 nm. A CPD of 0.5 V is the maximum theoretical contact potential difference that may be present between two metals [32]. In this case in order to avoid adhesive electrostatic forces an average arithmetic roughness of at least 25 nm should be applied to the contacting surface. If the sphere is made of aluminum instead of steel resulting in a smaller weight of the sphere, the arithmetic average roughness to apply should be increased in order for gravity to overcome the electrostatic forces.

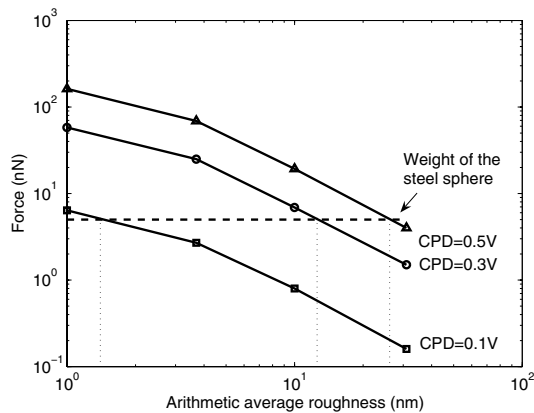


Fig. 10. Electrostatic normal force (nN) versus arithmetic average roughness (nm) for different applied voltages for a sphere of radius $R=25\mu\text{m}$ in contact with an infinite plane. Weight of the sphere is also represented for steel

V. CONCLUSION

We have developed a reliable simulation tool for electrostatic forces which can be used to design microgrippers and develop micromanipulations strategies in order to minimize the disturbing effects of adhesive electrostatic forces. Comparison of the results with analytical models allowed to demonstrate the reliability of the simulations. Simulations performed including surface topography representation showed the importance of surface roughness at very close separation distances. It also brought into light the need to find an accurate model for this surface topography. Ideally the model should be adapted to correlate the microfabrication process used for manufacturing the gripper. This is part of our prospective work. We also intend to perform experimental measures of the electrostatic forces in order to compare our simulations results with our own experimental measures after having characterized the roughness parameters of the sample.

REFERENCES

- [1] Y. Rollot, S. Régnier, and J. C. Guinot, "Simulation of micromanipulations: Adhesion forces and specific dynamic models," *Int. J. Adhes. Adhes.*, vol. 19, no. 1, pp. 35–48, 1999.
- [2] D. S. Haliyo, "Les forces d'adhésion et les effets dynamiques pour la micro-manipulation," Ph.D. dissertation, Université Pierre et Marie Curie, 2002.
- [3] P. Lambert and S. Régnier, "Surface and contact forces models within the framework of microassembly," *Journal of Micromechanics*, vol. 3, no. 2, pp. 123–157, 2006.
- [4] M. Gauthier, S. Régnier, P. Rougeot, and N. Chaillet, "Analysis of forces for micromanipulations in dry an dliquid media," *Journal of Micromechanics*, vol. 3, pp. 389–413, 2006.
- [5] R. S. Fearing, "Survey of sticking effects for micro parts handling," in *Proc. of IEEE/RSJ Conf. on Intelligent Robots and Systems*, 1995, pp. 212–217.
- [6] P. Lambert, "A contribution to microassembly: a study of capillary forces as a gripping principle," Ph.D. dissertation, Université libre de Bruxelles, Belgium, 2004.
- [7] B. Bhushan, "Adhesion and stiction: mechanisms, measurement techniques, and methods for reduction," *J. Vacuum Sci. Technol. B*, vol. 21, no. 6, pp. 2262–96, 2003.
- [8] Y. I. Rabinovich, J. J. Adler, M. S. Esayanur, A. Ata, R. K. Singh, and B. M. Moudgil, "Capillary forces between surfaces with nanoscale roughness," *Adv. Colloid Interface Sci.*, vol. 96, pp. 213–30, 2002.
- [9] W. M. van Spengen, I. De Wolf, and R. Puers, "An auto-adhesion model for mems surfaces taking into account the effects of surface roughness," in *Proc. of SPIE Conf. on Materials and Device Characterization in Micromachining III*, vol. 4175, 2000, pp. 104–112.
- [10] F. Arai, D. Ando, T. Fukuda, Y. Nonoda, and T. Oota, "Micro manipulation based on micro physics," in *Proc. of IEEE/RSJ Conf. on Intelligent Robots and Systems*, vol. 2, Pittsburgh, 1995, pp. 236–241.
- [11] B. Vögeli and H. von Känel, "AFM-study of sticking effects for microparts handling," *Wear*, vol. 238, no. 1, pp. 20–24, 2000.
- [12] M. Herman and K. Papadopoulos, "Effects on the van der waals and electric double layers interactions of two parallel flay plates," *J. Colloid Interface Sci.*, vol. 136, no. 2, p. 385, 1990.
- [13] L. Suresh and J. Walz, "Effect of surface roughness on the interaction energy between a colloidal sphere and a flat plate," *J. Colloid Interface Sci.*, vol. 183, pp. 199–213, 1996.
- [14] M. Kostoglou and A. Karabelas, "Effect of roughness on energy of repulsion between colloidal surfaces," *J. Colloid Interface Sci.*, vol. 171, pp. 187–199, 1995.
- [15] K. Komvopoulos, "Surface engineering and microtribology for micro-electromechanical systems," *Wear*, vol. 200, no. 1, pp. 305–327, 1996.
- [16] A. Majumdar and B. Bhushan, "Role of fractal geometry in roughness characterization and contact mechanics of surfaces," *J. Tribology*, vol. 112, pp. 205–216, 1990.
- [17] M. V. Berry and Z. V. Lewis, "On the Weierstrass-Mandelbrot fractal function," *Proc. R. Soc. London Ser. A*, vol. 370, pp. 459–84, 1980.
- [18] K. Komvopoulos, "A fractal analysis of stiction in microelectromechanical systems," *J. Tribology*, vol. 119, no. 3, pp. 391–400, 1997.
- [19] L. He and J. Zhu, "The fractal character of processed metal surfaces," *Wear*, vol. 208, pp. 17–24, 1997.
- [20] D. J. Whitehouse, "Fractal or fiction," *Wear*, vol. 249, no. 5-6, pp. 345–353, 2001.
- [21] A. G. S. Eichenlaub and S. Beaudouin, "Roughness models for particle adhesion," *J. Colloid Interface Sci.*, vol. 280, pp. 289–298, 2004.
- [22] S. Ganti and B. Bhushan, "Generalized fractal analysis and its applications to engineering surfaces," *Wear*, vol. 180, pp. 17–34, 1994.
- [23] A. Majumdar and C. Tien, "Fractal characterization and simulation of rough surfaces," *Wear*, vol. 136, pp. 313–327, 1990.
- [24] H. Zhu, S. Ge, X. Huang, D. Zhang, and J. Liu, "Experimental study on the characterization of worn surface topography with characteristic roughness parameter," *Wear*, vol. 255, pp. 309–314, 2003.
- [25] S. Belaidi, P. Girard, and G. Leveque, "Electrostatic forces acting on the tip in atomic force microscopy: modelization and comparison with analytic expressions," *J. Appl. Phys.*, vol. 81, no. 3, pp. 1023–1029, 1997.
- [26] B. Cappella and G. Dietler, "Force-distance curves by atomic force microscopy," *Surf. Sci. Rep.*, vol. 34, pp. 1–104, 1999.
- [27] H.-J. Butt, B. Cappella, and M. Kappl, "Force measurements with atomic force microscope: Technique, interpretation and applications," *Surf. Sci. Rep.*, vol. 59, pp. 1–152, 2005.

- [28] S. Hudlet, M. S. Jean, and J. Berger, "Evaluation of the capacitive force between an atomic force microscopy tip and a metallic surface," *Eur. Phys. J. B*, vol. 2, pp. 5–10, 1998.
- [29] H. W. Hao, A. M. Baro, and J. J. Saenz, "Electrostatic and contact forces in force microscopy," *J. Vacuum Sci. Technol. B*, vol. 9, no. 2, pp. 1323–8, 1991.
- [30] G. Sacha, A. Verdaguer, J. Martinez, J. Sáenz, D. Ogletree, and M. Salmeron, "Effective radius in electrostatic force microscopy," *Appl. Phys. Lett.*, vol. 86, p. 123101, 2005.
- [31] J. N. Israelachvili, "The nature of van der Waals forces," *Contemporary Physics*, vol. 15, no. 2, pp. 159–177, 1974.
- [32] R. A. Bowling, "A theoretical review of particle adhesion," in *Proc. of Symposium on particles on surfaces 1: Detection, Adhesion and Removal*, San Francisco, 1986, pp. 129–142.